Kalpa Publications in Computing

Volume 22, 2025, Pages 292–301

Proceedings of The Sixth International Conference on Civil and Building Engineering Informatics

Intelligent Design for Component Size of Reinforced Concrete Frame Structures using Diffusion Models

Yi Gu[1], Sizhong Qin[1], Wenjie Liao[2], Siqi Chen[1] and Xinzheng Lu[1,*]

[1] Tsinghua University, Beijing, China

[2] Southwest Jiaotong University, Chengdu, China

luxz@tsinghua.edu.cn

Abstract

The dimension design of components in reinforced concrete frame structures heavily relies on engineering experience and iterative calculations, leading to significant inefficiencies. Existing intelligent design methods struggle to conduct component size design because it is challenging to accurately and densely represent information such as component layout, dimensions, and design conditions. This study proposes a method for intelligent component size design based on feature space for accurate and dense representation of design information, as well as a diffusion design process constrained by multi-channel masks. Firstly, the method substitutes the feature space for the traditional RGB space to represent component layout, dimensions, and design conditions, thereby enhancing data representation and neural network learning capabilities. Secondly, the study introduces an image-guided diffusion model with multi-channel mask tensors, and the corresponding training method is derived. Experimental results demonstrate that this model exhibits strong feature extraction capabilities and performs well in component dimension design tasks. Lastly, the study discusses the impact of parameters such as multi-channel masks and different dataset construction methods on the final prediction results.

1 Introduction

Reinforced concrete (RC) frame structures are widely used in modern structural engineering, with the design of sectional dimensions being of significant importance for ensuring structural safety, cost-effectiveness, and environmental sustainability (Zhang et al., 2024). However, the traditional design process typically relies on the experience of structural engineers, leading to a high level of subjectivity and uncertainty in the design outcomes (Qin et al., 2024; Liao et al., 2024).

I. Hkust, J. Cheng and Y. Yantao (eds.), ICCBEI 2025 (Kalpa Publications in Computing, vol. 22), pp. 292–301

Traditional intelligent design methods for frame structure component dimension mainly consist of various optimization methods. Heuristic algorithms, such as genetic algorithms (Mariniello et al., 2022; Trapani et al., 2022; Xu and Gong, 2001), simulated annealing (Li et al., 2010), particle swarm optimization, artificial bee colony algorithm (Kaveh et al., 2020), are widely used in the optimization of RC frame component dimensions. These traditional optimization methods, especially in the application of complex structural design, are constrained by the design space scale and solution efficiency (Chang and Cheng, 2020). For example, heuristic algorithm-based optimization methods, while capable of providing effective solutions in certain scenarios, come with a significant computational burden, making it challenging to meet the design requirements of large RC frame structures (Peng et al., 2021). Additionally, the complexity of RC structures lies in the interactions between components and load effects, leading to highly nonlinear and coupled features in the design space (Trapani et al., 2022). The layout and section design of beams, columns, and slabs must comprehensively consider the influence of seismic loads, vertical loads, and other external factors (Xu et al., 2018). These complexities further compound the challenges posed by traditional design methods.

The emergence of models such as Generative Adversarial Networks (GANs) and Graph Neural Networks (GNNs) has introduced new methods for automated and efficient structural design. These algorithms, which learn from existing design drawings, can capture implicit knowledge in structural design. In comparison to traditional optimization algorithms, they have demonstrated significant improvements in both computational efficiency and design rationality. In recent years, the Diffusion Model has garnered attention in the field of structural engineering as an emerging generative model. The Diffusion Model operates by simulating data from high noise to low noise in a reverse process to gradually produce high-quality images (Ho et al., 2020). However, existing studies have primarily concentrated on shear wall layout design. To the best of the authors' knowledge, there is currently no method available for the dimension design of RC frame components based on the Diffusion Model.

In conclusion, the optimization of the dimension design of RC frame components encounters challenges stemming from the highly nonlinear space of traditional methods, the fitting limitations of GNN, and the sparse feature representation in GAN and Diffusion Models. Building on these identified challenges, this study seeks to investigate the utilization of the Diffusion Model in the dimension design of RC frame components. Through the integration of multi-channel masks, a design method is proposed that densely considers the features of beam, slab, and column components. Specifically, the contributions of this study include the following points:

a) A dimension design method for RC frame components based on the Diffusion Model is proposed, which enhances the model's accuracy by introducing multi-channel masks.

b) A dataset construction method suitable for the dimension design of RC frame components is developed, taking into account story-related features such as story height and building-related features such as seismic design acceleration, and integrating multi-standard story information for the Diffusion Model learning.

The subsequent organization of this paper is as follows: Section 2 will provide an overview of the overall methodology, Section 3 will detail the construction method of the dataset; Section 4 will introduce the model architecture and its implementation details; Section 5 will discuss the impact of various factors on the generation effectiveness of the Diffusion Model. Finally, Section 6 will present the conclusion of this study.

2 The Diffusion-based Component Dimension Design Method for RC Frame Structures

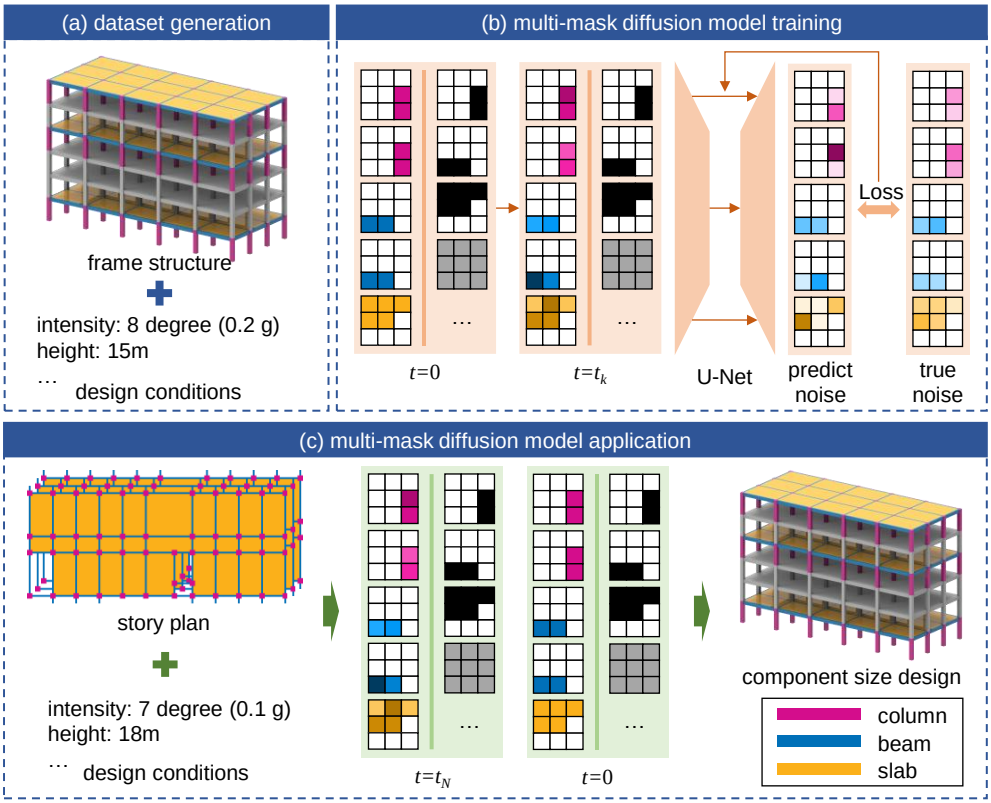

Figure 1: Diffusion-based design method for component size of RC frame structures. (a) dataset generation, (b) multi-mask diffusion model training, and (c) multi-mask diffusion model application.

This study introduces a dimension prediction method for RC frame components based on the diffusion process, named Frame-dimension-diffusion. As illustrated in Figure 1, the proposed method comprises three main components: (a) dataset generation, (b) multi-mask diffusion model training, and (c) multi-mask diffusion model application.

(a) Dataset generation (Figure 1(a)): A novel representation method for RC frame structures is introduced in this section to align with the input and output requirements of the diffusion model. In this study, the RC frame structure is represented layer by layer as images, with each image containing multiple channels representing information on component dimensions, layout, or design conditions. Based on the proposed structural representation method, this study extensively explores dataset construction, the incorporation of design conditions, and techniques for data augmentation, as outlined in Section 3.

(b) Multi-mask diffusion model training (Figure 1(b)): Gu et al. (2024) introduced a mask-based shear wall generation model, Struct-diffusion, which improved the density of shear wall structure data representation in images. This study extends the concept by proposing a diffusion model incorporating multi-channel masks. This approach mitigates the challenge of inadequate prediction performance for components with limited pixel proportions. The specific training process of the

diffusion model will be presented in Section 4, with the benefits of the multi-channel masks discussed in Section 5.

(c) Multi-mask diffusion model application (Figure 1(c)): Based on the training method outlined above, a dimension design model for RC frame components is obtained, enabling a more precise generation of RC frame component dimensions. The process for predicting the dimensions of frame components through the model is depicted in Figure 1(c). The detailed inference process of the diffusion model will be presented in Section 4.

3 Dataset Generation

The architectural design information of frame structures can be conveniently processed into structured data (Chang and Cheng, 2020). The utilization of text-prompt methods may not provide direct guidance and can result in redundant information. Therefore, this study adopts an image-prompt method to guide the diffusion process (Gu et al., 2024). Moreover, the generation strategy of Stable Diffusion mainly focuses on producing the complete image (Rombach et al., 2022). However, in practice, the pixel count occupied by frame columns and beams is considerably smaller than the total pixel count in the image ($O(1)<<O(N) << O(N^2)$, where N represents the number of pixels on the longer side of the image). Therefore, using the full-image generation approach directly would result in significant inefficiency and could introduce biases during neural network training. Additionally, unlike the shear wall design task in Struct-diffusion, there are notable variations in the number of pixels occupied by beams, columns, and slabs. Therefore, a tailored multi-channel mask method needs to be devised. Based on the above content, this section will delve into the dataset construction method.

3.1 Method of Dataset Construction

Each standard story is regarded as a data point for analysis in this study. For each story, the method shown in Figure 2, as recommended by Han et al. (2024), was employed to encode features in the feature space and alleviate the impact of erroneous priors on the model. This study categorizes features into two groups: story-related features, demonstrated in Figure 2(a), and building-related features, illustrated in Figure 2(b). Story-related features may vary between different standard stories, such as the dimensions of beams, columns, and slabs, the arrangement of beams, columns, and slabs, loads on slabs, story heights, story numbers, etc. Building-related features, on the other hand, remain consistent within the same building, such as the total number of stories in the building, seismic design acceleration, characteristic period of the site, frame seismic resistance grade, etc.

The specific method entails transforming the current dimensions of frame components into pixelated story plans. In this study, the image pixels are configured at 256 × 256, with a scaling ratio of 1 px = 300 mm between the image and the drawings. Due to the small dimension of most components after scaling by this ratio, which is not conducive for AI training, all columns are denoted by 3 × 3 pixel rectangles, while beams are fixed as 1-pixel-wide rectangles. It is crucial to highlight that adjusting the 1 px = 300 mm scale ratio does not significantly affect this study, as it does not pertain to layout design. The key criterion is ensuring each component can be distinctly identified on the drawing.

After converting into pixelated story plans, dimension information is allocated to the component locations channel by channel, constructing the corresponding tensors. Figure 2(a) illustrates an example within a 3 × 3 pixel range. Here, column lx signifies the column width in the x-direction (measured in mm), while column ly denotes the column width in the y-direction (measured in mm). It is essential to clarify that in this study, the x and y directions do not align with the strong and weak axes of the structure but rather with the local coordinate system of the columns. For non-rectangular

columns like circular or pentagonal columns, are approximated as rectangular columns following engineering conventions. The interpretations of beam height, beam width, and slab thickness tensors are self-evident. The column mask, beam mask, and slab mask indicate the positions of columns, beams, and slabs, where a value of 1 signifies the presence of the corresponding component at that pixel point, while 0 denotes absence. The load tensor embodies the building loads, with values sourced from the Load Code for the Design of Building Structures (MOHURD, 2012). Scalar values such as story height and story number in Figure 2(a), as well as concrete material grade, total number of stories in the building, seismic design acceleration, characteristic period of site, and frame seismic resistance grade in Figure 2(b), which are independent of component positions, are directly expanded into 256 × 256 tensors. These tensors collectively constitute the feature tensors delineating the RC frame structure.

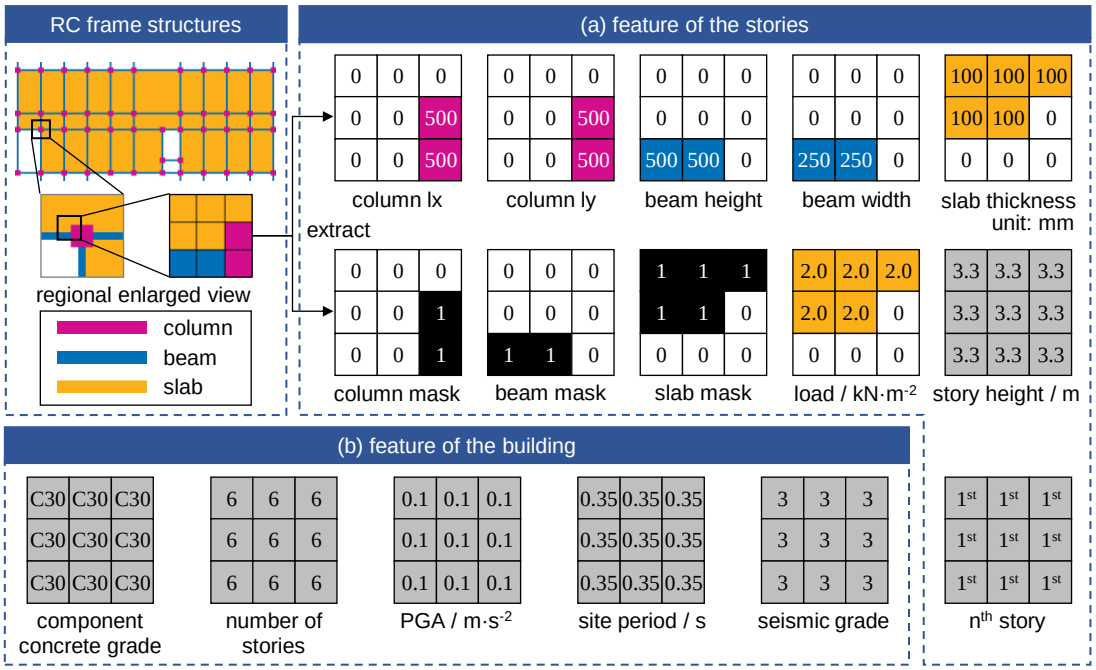

Figure 2: Representation of RC frame structures. (a) feature of the stories, and (b) feature of the building.

3.2 Data Augmentation

The dataset utilized in this study is an enhanced version of the dataset introduced by Qin et al. (2024). The dataset comprises 109 buildings, with a total of 380 standard stories. The dataset is segmented into training, validation, and testing sets, with the precise allocation detailed in Table 1. To avert data leakage, the standard stories of the test buildings in dataset are ensured to be excluded from the training or validation sets.

Table 1: Dataset split

Type	Datasets size
Train & Validation (K-fold)	362
Test	18

To address the limited number of training samples about the parameters of the diffusion model, data augmentation methods were also incorporated in this study to increase the amount of training data. The data augmentation techniques employed primarily encompass horizontal flipping, vertical flipping, and translation transformations to maintain the features of the training samples. By utilizing data augmentation techniques (Shorten and Khoshgoftaar, 2019), a training and validation dataset that is 196 times larger than the original dimension (= 4 × 7 × 7) was generated. This is beneficial for the training of the diffusion model.

4 The Architecture of the Neural Network Model

4.1 The Derivation of the Image-prompt Diffusion Model with Multi-mask Tensor

The diffusion model primarily consists of a forward diffusion process and a reverse denoising process. As Equation 1, the forward diffusion process is a Markov process where Gaussian noise is added at each step (Ho et al., 2020):

$$q(y_t|y_{t-1}) = \mathcal{N}\left(y_t; \sqrt{1-\beta_t}y_{t-1}, \beta_t I\right), q(y_{1:T}|y_0) = \prod_{t=1}^{T} q(y_t|y_{t-1}) \tag{1}$$

where β_t are hyperparameters of the noise schedule, y_t are input tensor in time *t*, *t*=0, 1, 2, 3, …, *T*, *T* is the time steps of the diffusion model, $q(x|y)$ means the conditional probability distribution of *x* given *y*, $\mathcal{N}(x; \mu; \sigma^2 I)$ means a multivariate normal distribution with a vector mean of μ and a covariance matrix of $\sigma^2 I$. In this study, *T*=2000, and the noise schedule is linear, which means that β_t varied linearly from 0.000001 to 0.01 (Dhariwal and Nichol, 2021). When $t = T$, there is no distinction between y_T and Gaussian noise. It is noteworthy that we can obtain the Equation 2:

$$q(y_t|y_0) = \mathcal{N}\left(y_t; \sqrt{\bar{\alpha}_t}y_0, (1-\bar{\alpha}_t)I\right) \tag{2}$$

where $\alpha_t = 1 - \beta_t, \bar{\alpha}_t = \prod_{i=1}^{t} \alpha_i$. $\bar{\alpha}_t$ actually measures the noise level, meaning that a smaller $\bar{\alpha}_t$ indicates that the image contains more noise. Ho et al. (2020) show a closed form of the posterier distribution of y_{t-1} given (y_0, y_t) as

$$q(y_{t-1}|y_0, y_t) = \mathcal{N}\left(y_{t-1}; \frac{\sqrt{\alpha_t}(1-\bar{\alpha}_{t-1})}{1-\bar{\alpha}_t}y_t + \frac{\sqrt{\bar{\alpha}_{t-1}}}{1-\bar{\alpha}_t}\beta_t y_0, \frac{1-\bar{\alpha}_{t-1}}{1-\bar{\alpha}_t}\beta_t I\right). \tag{3}$$

Based on the work of Gu et al. (2024) and Ho et al. (2020), this study additionally incorporates a multi-mask tensor. Given a noisy tensor $\tilde{y}_t = \tilde{y}_{bh,t} \oplus \tilde{y}_{bw,t} \oplus \tilde{y}_{cx,t} \oplus \tilde{y}_{cy,t} \oplus \tilde{y}_{st,t}$:

$$\begin{aligned} &\tilde{y}_{k,t} = \left(\sqrt{\bar{\alpha}_t}y_{k,0} + \sqrt{1-\bar{\alpha}_t}\varepsilon_{k,t}\right) \odot y_{k\_mask} + y_0 \odot \left(1 - y_{k\_mask}\right), \varepsilon_{k,t} \sim \mathcal{N}(0, I), k \\ &\in \{bh, bw, cx, cy, st\}; \\ &y_{bh\_mask} = y_{bw\_mask} = y_{beam\_mask};\ y_{cx\_mask} = y_{cy\_mask} = y_{column\_mask}; y_{st\_mask} \\ &= y_{slab\_mask} \end{aligned} \tag{4}$$

where $\tilde{y}_{bh,t}$ means beam height channel of noisy tensor $\tilde{y}_t$. bw means beam width, cx means column lx, cy means column ly, and st means slab thickness, $\oplus$ means concatenate operator. We denote $y_{mask} = y_{beam\_mask} \oplus y_{beam\_mask} \oplus y_{column\_mask} \oplus y_{column\_mask} \oplus y_{slab\_mask}$. The goal is to recover the target tensor $y_0 \odot y_{mask}$, where $\odot$ is the hadamard product operator. A neural network $M_\theta(y_{cond}, \tilde{y}_t, \bar{\alpha}_t)$ can be constructed, which takes condition tensor y_{cond}, input tensor with noise $\tilde{y}_t$ and noise level $\bar{\alpha}_t$ as input and fits the noise vector ε by optimizing the objective

$$\mathbb{E}_{(y_0, y_{cond}, y_{mask})}\, \mathbb{E}_{\bar{\alpha}, \varepsilon}\left[\|(M_\theta(y_{cond}, \tilde{y}_t, \bar{\alpha}_t) - \varepsilon_t) \odot y_{mask}\|_p^p\right]. \tag{5}$$

Based on this, the process of training the denoising diffusion model can be obtained, as outlined in Table 2. The inference process is the same as Struct-diffusion.

Table 2: The process of denoising diffusion model training and inference

Algorithm 1 Training

repeat
  $y_{cond}, y_0, y_{mask} \sim q(y_{cond}, y_0, y_{mask})$
  $t \sim \text{Uniform}(\{1, \dots, T\})$
  $\varepsilon \sim \mathcal{N}(0, I)$
  Take gradient descent step on
  $$\nabla_\theta \left\| \left(M_\theta \left(y_{cond}, \left(\sqrt{\bar{\alpha}_t} y_0 + \sqrt{1-\bar{\alpha}_t}\varepsilon \right) \odot y_{mask} + y_0 \odot (1 - y_{mask}),\ \bar{\alpha}_t \right) - \varepsilon_t \right) \odot y_{mask} \right\|^2$$
until converged

Algorithm 2 Inference

$z \sim \mathcal{N}(0, I)$
$\hat{y}_T \leftarrow z \odot y_{mask} + y_0 \odot (1 - y_{mask})$
for $t = T, \dots, 1$ **do**
  $z \sim \mathcal{N}(0, I)$ if $t > 1$, else $z = 0$
  $$\hat{y}_{t-1} \leftarrow \left(\frac{1}{\sqrt{\alpha_t}} \left(\hat{y}_t - \frac{1-\alpha_t}{\sqrt{1-\bar{\alpha}_t}} M_\theta (y_{cond}, \hat{y}_t, \bar{\alpha}_t) \right) + \sqrt{\beta_t} z \right) \odot y_{mask} + y_0 \odot (1 - y_{mask})$$
end for
return $\hat{y}_0$

It is worth noting that when $y_{beam\_mask} = y_{column\_mask} = y_{slab\_mask} = y_{mask}$, this method degenerates to Struct-diffusion. In this study, we consider $y'_{beam\_mask} = y'_{column\_mask} = y'_{slab\_mask} = y_{beam\_mask} \mid y_{column\_mask} \mid y_{slab\_mask}$ as a single mask scenario, where $y_{beam\_mask}, y_{column\_mask}, y_{slab\_mask}$ represent the layout of beams, columns, and slabs obtained in Section 3.1.

4.2 Training Details

This study employed a U-Net network with an attention mechanism and temporal encoding (Dhariwal and Nichol, 2021) as the denoising model. To investigate the impact of the various factors mentioned above on the model results, this study conducted two sets of training. The specific training IDs and corresponding model parameters can be found in Table 3. In the table, the ID column represents the name of the trained model. The ID names are designated based on the presence of multi-channel masks. For example, for model with multi-channel masks, the model ID is labeled as M. Here, "M" stands for Multi-mask, and "S" stands for Single-mask. The term Epoch denotes the number of training cycles, whereas Epoch 21600 signifies a total of 21600 training cycles. The Seed indicates the chosen random seed, which controls processes such as neural network weight initialization and Gaussian noise sampling. If the random seeds are the same, it indicates identical outcomes for these processes. It is crucial to mention that each set of training has three random seeds, indicating that each set underwent three training runs to reduce the impact of random errors on the research conclusions. The Training hours column represents the total training time. Further explanations on Mask type is provided in Section 4.1.

Table 3: Training details

ID	Epoch	Seed	Training hours	Mask type
S	6400	42, 88, 8888	58.30	Single
M	11200	42, 88, 8888	110.00	Multi

The training strategy for the aforementioned experiments was consistently maintained, wherein the models were trained with a learning rate of 5 × 10-5 following optimization of other hyperparameters. Mean square error calculation was employed for both training and validation processes. Validation error assessment occurred every 200 Epochs, and training concluded after 30 consecutive validations without enhancement. The model with the minimal validation error was chosen for prediction and subsequent metric computations. Furthermore, to ensure model reproducibility, the random seed specified in Table 3 governed the model's random initialization, irrespective of the dataset splitting methodology. To ensure equitable comparisons, the dataset-splitting method remained uniform. Table 3 also presents the training duration of the models (on a single GPU, measured in hours). The computing platform configuration included OS: Ubuntu 22.04 LTS; CPU: Intel Xeon E5-2682 v4 @ 64x 3GHz; RAM: 32GB; GPU: NVIDIA GeForce RTX 3090 24GB.

5 Discussion

5.1 Evaluation Metrics and Postprocessing

Following the methodology proposed by Qin et al. (2024), this study employed the Root Mean Square Error (RMSE) metric for evaluation. The metric calculates the root mean square error between the results obtained from the diffusion model design and the engineering design (Ground Truth, GT). The reason for choosing this metric is that it maintains the same units as the original data, allowing for a direct assessment of the variability in the corresponding predicted results. In this study, we primarily compared the RMSE values for beam height, beam width, column length in the x-direction, column length in the y-direction, and slab thickness. It is noteworthy that in practical design, the modulus is often applied. For instance, if the designed beam width is 195mm, it might be rounded up to 200mm. Typically, the modulus for beams and columns is 50mm, while for slabs, it is 20mm.

For the predictions produced by the diffusion model, the average value of the respective channel for each component was extracted to acquire the dimensional details of that component. Subsequently, by consolidating all the dimensional information of the building, the RMSE was computed as the evaluation metric in this study. Hence, the RMSE is component-centric rather than pixel-centric, aligning with real-world applications.

5.2 Test Results

Using the RMSE metric provided in Section 5.1, the two sets of models shown in Table 3 were tested, and Table 4 presents the average performance of these models on the prediction dataset. Each column in the table represents the model's ID, as well as the RMSE values for beam width, beam height, column length in the x-direction, column length in the y-direction, and slab thickness, all measured in millimeters.

Table 4: RMSE error on the Test dataset (unit: mm)

ID	Beam height	Beam width	Column lx	Column ly	Slab thickness
S	152.0696	44.4171	122.5505	128.0622	13.5619
M	**114.3256***	**32.4199***	**62.6379***	**76.3565***	**13.3414***

Comparing the results of IDs S with M, it can be observed that the multi-channel masks outperform the single-channel masks. In the case of column and beam channels, the absence of multi-channel masks leads to a high number of zero values, significantly surpassing the valid values. This scenario can mislead the neural network during backpropagation, as it may predict the positions

directly as zeros, thereby causing larger prediction errors. Additionally, it is noticeable that the improvement in prediction errors for slabs is relatively minor compared to beams and columns, which aligns with the aforementioned discussion.

5.3 Summary

This section analyzed the impact of various factors on the results generated by the diffusion model. Among them, the model utilizing multi-channel masks achieved the best performance. Furthermore, the top-performing model had all dimension predictions within two modulus, except for beam height prediction which was within three modulus. It can be concluded that this method is suitable for predicting the dimension of RC frame components.

6 Conclusion

This study introduces a novel diffusion model-based approach for predicting component dimensions in RC frame structures, effectively addressing the limitations of traditional heuristic methods and GAN-based approaches in capturing the nonlinear and coupled features of structural design. By integrating multi-channel masking, the proposed Frame-dimension-diffusion model offers a more robust and precise prediction of beam, column, and slab dimensions. The principal contributions of this research are as follows:

(a) A novel framework based on diffusion models has been developed specifically to predict the component dimensions of RC frames. This approach leverages advanced generative modeling techniques inherent to diffusion processes, enabling more precise estimations of component dimensions.

(b) The framework incorporates multi-channel masks to improve feature representation for individual components. By applying this technique, the model achieves higher density and accuracy in capturing the nuanced features of RC frame components.

(c) A novel dataset construction methodology is proposed, capturing key characteristics of standard stories and building seismic conditions, thereby enhancing the training process and efficacy of the diffusion model.

The findings indicate that the Frame-dimension-diffusion model is capable of generating component dimensions that comply with engineering standards, exhibiting reduced prediction error. Future research should focus on improving model efficiency through advanced architectural techniques, such as model distillation, and incorporating spatial layout information to extend the diffusion model's applicability to more complex structural design scenarios.

Acknowledgement

This work was supported by the Ministry of Housing and Urban-Rural Development of the People's Republic of China, Science and Technology Program (2022-K-073).

References

Chang, K.-H., Cheng, C.-Y., 2020. Learning to Simulate and Design for Structural Engineering, in: Proceedings of the 37th International Conference on Machine Learning. Presented at the International Conference on Machine Learning, PMLR, pp. 1426–1436.

Dhariwal, P., Nichol, A., 2021. Diffusion Models Beat GANs on Image Synthesis. https://doi.org/10.48550/arXiv.2105.05233

Gu, Y., Huang, Y.L., Liao, W.J., Lu, X.Z., 2024. Intelligent design of shear wall layout based on diffusion models. Computer-Aided Civil and Infrastructure Engineering. https://doi.org/10.1111/mice.13236

Han, J., Lu, X.Z., Gu, Y., Liao, W.J., Cai, Q., Xue, H.J., 2024. Optimized data representation and understanding method for the intelligent design of shear wall structures. Engineering Structures 315, 118500. https://doi.org/10.1016/j.engstruct.2024.118500

Ho, J., Jain, A., Abbeel, P., 2020. Denoising Diffusion Probabilistic Models. https://doi.org/10.48550/arXiv.2006.11239

Kaveh, A., Hamedani, K.B., Hosseini, S.M., Bakhshpoori, T., 2020. Optimal design of planar steel frame structures utilizing meta-heuristic optimization algorithms. Structures 25, 335–346. https://doi.org/10.1016/j.istruc.2020.03.032

Li, G., Lu, H.Y., Liu, X., 2010. A hybrid simulated annealing and optimality criteria method for optimum design of RC buildings. Structural Engineering and Mechanics 35, 19–35. https://doi.org/10.12989/sem.2010.35.1.019

Liao, W.J., Lu, X.Z., Fei, Y.F., Gu, Y., Huang, Y.L., 2024. Generative AI design for building structures. Automation in Construction 157, 105187. https://doi.org/10.1016/j.autcon.2023.105187

Mariniello, G., Pastore, T., Bilotta, A., Asprone, D., Cosenza, E., 2022. Seismic pre-dimensioning of irregular concrete frame structures: Mathematical formulation and implementation of a learn-heuristic algorithm. Journal of Building Engineering 46, 103733. https://doi.org/10.1016/j.jobe.2021.103733

MOHURD, 2012. Load Code for the Design of Building Structures (GB 50009-2012).

Peng, B., Flager, F., Barg, S., Fischer, M., 2021. Cost-based optimization of steel frame member sizing and connection type using dimension increasing search. Optimization and Engineering 23, 1525–1558. https://doi.org/10.1007/s11081-021-09665-5

Qin, S.Z., Liao, W.J., Huang, Y.L., Zhang, S.L., Gu, Y., Han, J., Lu, X.Z., 2024. Intelligent Design for Component Size Generation of Reinforced Concrete Frame Structures Using Heterogeneous Graph Neural Networks. Automation in Construction.

Rombach, R., Blattmann, A., Lorenz, D., Esser, P., Ommer, B., 2022. High-Resolution Image Synthesis with Latent Diffusion Models. https://doi.org/10.48550/arXiv.2112.10752

Shorten, C., Khoshgoftaar, T.M., 2019. A survey on Image Data Augmentation for Deep Learning. Journal of Big Data 6, 60. https://doi.org/10.1186/s40537-019-0197-0

Trapani, F.D., Sberna, A.P., Marano, G.C., 2022. A genetic algorithm-based framework for seismic retrofitting cost and expected annual loss optimization of non-conforming reinforced concrete frame structures. Computers & Structures 271, 106855. https://doi.org/10.1016/j.compstruc.2022.106855

Xu, L., Gong, Y.L., 2001. Preliminary Design of Long-Span King-Post Truss Systems with a Genetic Algorithm. Computer-Aided Civil and Infrastructure Engineering 16, 94–105. https://doi.org/10.1111/0885-9507.00216

Xu, L.H., Yan, X.T., Li, Z.X., 2018. Development of BP-based seismic behavior optimization of RC and steel frame structures. Engineering Structures 164, 214–229. https://doi.org/10.1016/j.engstruct.2018.03.012

Zhang, C., Tao, M.X., Wang, C., Yang, C., Fan, J.S., 2024. Differentiable automatic structural optimization using graph deep learning. Advanced Engineering Informatics 60, 102363. https://doi.org/10.1016/j.aei.2024.102363